JBMR Plus, 2024, **8**, ziae036
https://doi.org/10.1093/jbmrpl/ziae036
Advance access publication: April 6, 2024
Research Article

MiR-144-5p and miR-21-5p do not drive bone disease in a mouse model of type 1 diabetes mellitus

Souad Daamouch[1], Matthias Blüher[2], David Carro Vázquez[3], Matthias Hackl[3], Lorenz C. Hofbauer[1], Martina Rauner[1,*]

[1]Department of Medicine III, Center for Healthy Aging, Technische Universität Dresden, Dresden, Saxony, 01307, Germany
[2]Helmholtz Institute for Metabolic, Obesity and Vascular Research (HI-MAG) of the Helmholtz Zentrum München at the University of Leipzig and University Hospital Leipzig, Leipzig, Saxony, 04109, Germany
[3]TAmiRNA, Vienna, 1110, Austria
*Corresponding author: Martina Rauner, Department of Medicine III & Center for Healthy Aging, Medical Faculty of the TU Dresden, Fetscherstraße 74, Dresden 01307, Germany (Martina.Rauner@ukdd.de).

Abstract

The increased risk of fractures in patients with type 1 diabetes mellitus (T1DM) is nowadays well recognized. However, the exact mechanism of action of diabetic bone disease has not been fully elucidated. MicroRNAs (miRNAs) are gene regulators that operate post-transcriptionally and have been implicated in the development of various metabolic disorders including T1DM. Previous studies have implicated a role for miR-144-5p and miR-21-5p, which are involved in controlling oxidative stress by targeting Nrf2, in T1DM. To date, it is unclear whether miR-144-5p and miR-21-5p affect bone health in T1DM. Thus, this study aimed to investigate the influence of miR-144-5p and miR-21-5p knockdown in the development of bone disease in T1DM male mice. Therefore, T1DM was induced in 10-wk-old male mice using streptozotocin (STZ). One week later, after development of hyperglycemia, antagomir-144-5p and antagomir-21-5p or their non-targeting control were administered at 10 mg/kg BW once a week until the end of the experiment. At 14 wk of age, glucose levels, bone, and fat mass were analyzed. The results revealed that treating T1DM male mice with antagomir-144-5p and antagomir-21-5p did not protect against diabetes development or bone loss, despite the successful downregulation of the miRNAs and the normalization of Nrf2 mRNA levels in bone tissue. Histological and serological parameters of bone formation or resorption were not altered by the antagomir treatment. Finally, we measured the expression of miRNA-144-5p or miRNA-21-5p in the serum of 30 individuals with T1DM and compared them to non-diabetic controls, but did not find an altered expression of either miRNA. In conclusion, the knockdown of miR-144-5p and miR-21-5p does not affect STZ-induced diabetes development or loss of bone mass in male mice. However, it does normalize expression of the anti-oxidant factor Nrf2 in diabetic bone tissue.

Keywords: miR-144-5p, miR-21-5p, antagomir, bone loss, T1DM

Lay Summary

People with type 1 diabetes mellitus (T1DM) are more prone to fractures, but the underlying mechanisms of diabetic bone disease remain unclear. In this study, we looked at tiny molecules called microRNAs (miRNAs), specifically miR-144-5p and miR-21-5p, which play a role in controlling oxidative stress in T1DM. We studied male mice with T1DM to see if blocking these miRNAs would help their bone health. Even though we successfully reduced these miRNAs and brought Nrf2 levels back to normal in the bone tissue, it did not prevent diabetes or bone loss in the mice. When we checked the serum of patients with T1DM, we did not find any significant differences in these miRNA levels compared to those without diabetes. In summary, blocking miR-144-5p and miR-21-5p did not stop T1DM or bone loss in mice, but it did normalize Nrf2 expression in diabetic bone tissue.

Received: October 10, 2023. **Revised:** March 1, 2024. **Accepted:** March 4, 2024

Graphical Abstract

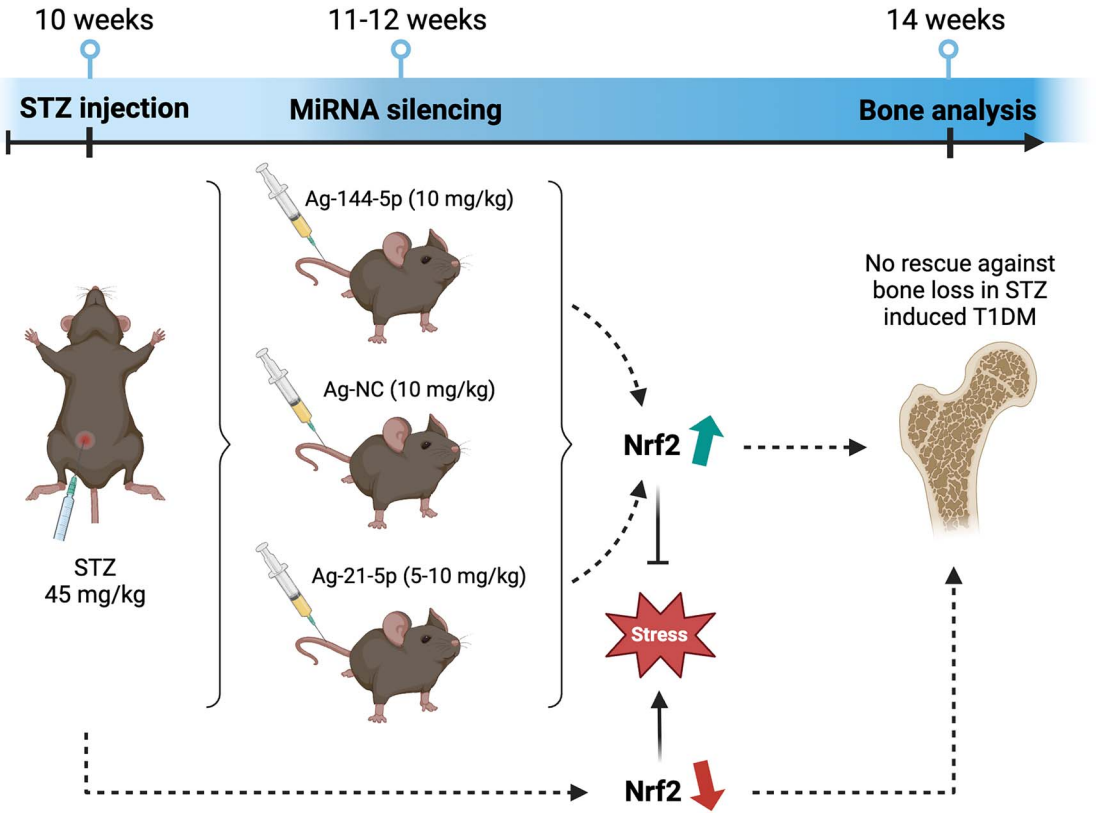

Introduction

Type 1 diabetes mellitus (T1DM) is an autoimmune disease that has witnessed a rise in its prevalence in recent years, affecting over 8 million people worldwide in 2022 according to the International Diabetes Federation.[1,2] This metabolic disorder is characterized by the destruction of pancreatic β-cells, leading to hyperglycemia.[3] Although T1DM is commonly diagnosed in childhood, with nearly 80% of β-cells already destroyed at that stage, there is a growing trend of diagnosis in young adults as well.[4-7] The insidious progression of the disease is associated with various complications such as cardiomyopathy, nephropathy, retinopathy, and bone loss leading to osteoporosis and an increased risk for fractures.[8-11]

Previous research has indicated the significant impact of miRNAs on T1DM-induced osteoporosis.[12] MicroRNAs, known as post-transcriptional gene regulators,[13,14] have been found to be dysregulated in patients with T1DM[15-17] and in patients with osteoporosis,[18,19] potentially contributing to impaired bone health. Previous studies have identified an upregulation of miR-144-5p[20] and miR-21-5p,[21,22] among other miRNAs, in patients with T1DM. As T1DM is an autoimmune condition, it generates oxidative stress and releases pro-inflammatory cytokines that impair bone metabolism, thereby increasing the fracture risk for patients with T1DM. Interestingly, these 2 miRNA candidates have been closely associated with oxidative stress and involved in ROS homeostasis by controlling the expression of nuclear factor erythroid 2–related factor 2 (Nrf2).[23-28] Under normal conditions, Nrf2 associates with Kelch-like ECH-associated protein 1 (Keap1) in the cytoplasm where it is kept inactive. Under oxidative stress, Keap1 dissociates from Nrf2, allowing it to translocate to the nucleus and to activate cytoprotective genes, including heme oxygenase-1 (Hmox1) and superoxide dismutase-1 (Sod1) to protect from oxidative damage.[29,30] Indeed, enhancing Nrf2 signaling has been demonstrated to offer protection against diabetes onset; for instance, in mice with Keap1-knockdown, increased Nrf2 signaling suppressed insulitis and protected against the autoimmune progression of T1DM mice.[31,32] Moreover, pharmacological activation of Nrf2 prevented bone loss due to various oxidative stressors (eg, hydrogen peroxide, diabetes, glucocorticoid excess) via preventing osteoblast apoptosis and the stimulation of osteoclasts.[33-37] Along those lines, enhanced expression of miR-144-5p under high-fat diet-induced type 2 diabetic conditions has been shown to impair fracture healing in male rats.[38]

The rationale to specifically study miR-144-5p and miR-21-5p is based on the hypothesis that silencing these miRNA targets on Nrf2 signaling could provide insights into their roles in diabetic bone disease. Therefore, based on the close association of miR-144-5p and miR-21-5p with oxidative stress through the Nrf2 signaling pathway, and their potential role in bone health in T1DM, we aimed to investigate their role in the development of T1DM bone disease in mice. Thus, we believe that impaired glucose and impaired insulin levels might be responsible for the development of oxidative stress, although it is possible that apoptotic beta cells could elicit an oxidative stress response. To that end, we systemically inhibited miR-144-5p and miR-21-5p using an antagomir-mediated approach in streptozotocin (STZ)-induced T1DM mice. Our data demonstrate that silencing miR-144-5p and miR-21-5p has no effect on STZ-induced hyperglycemia or

bone disease in T1DM mice, despite their ability to restore suppressed Nrf2 signaling in diabetic bone.

Materials and methods

STZ-induced T1DM mouse model

To establish our inducible T1DM mouse model, we initiated the experiment by administering a low concentration of STZ at 45 mg/kg via intra-peritoneal injections to male wild-type C57BL/6 J mice when they reached 10 wk of age. This treatment was performed consecutively for 5 d. As a control group, another set of mice received citrate buffer (CB) injections[39] (Figure 1). One week following the STZ or CB administrations, we measured blood glucose levels from the tail vein. Mice were considered to have developed diabetes when their blood glucose levels reached approximately 250 mg/dL. During establishment of the model, we observed that female mice did not develop T1DM using this dose of STZ. Thus, we only used male mice. The combined rate of mice not developing diabetes at the measurement of 1 wk was approximately 18%. T1DM male mice were not treated with insulin in this study. Throughout the study, we monitored blood glucose levels and body weight on a weekly basis until week 14, at which point all mice were euthanized. To maintain consistent conditions, all mice were provided with standard diets and had unrestricted access to water. They were housed in groups of 4 or 5 per cage, maintained at room temperature, and subjected to a 12-hour light/dark cycle. All mouse procedures were approved by the Landesdirektion Sachsen and in the institutional animal care committee.

Intravenous administration of antagomirs 144-5p and 21-5p

To knockdown miR-144-5p and miR-21-5p, we injected antagomir-144-5p (Ag-144-5p) and antagomir-21-5p (Ag-21-5p) re-suspended with PBS solution into the tail vein of diabetic mice. We started the treatment 1 wk after inducing diabetes in the mice using STZ injections. At this time, all mice had developed hyperglycemia. The dosage used was 10 mg/kg of body weight, and the antagomirs treatments were administered once a week. The injections were continued until the mice reached 14 wk of age, which marked the end of the experiment. As a comparison, the control groups of diabetic and non-diabetic mice received a scrambled antagomir treatment, as a negative control (NC). A NC is defined to have no hits of >70% homology to any sequence in any organism in the National Center for Biotechnology Information (NCBI) and miRbase databases. It serves as a crucial control to account for any non-specific effects in our experimental setup. All antagomirs (miRCURY LNA miRNA Inhibitors) were obtained from Qiagen and prepared following the manufacturer's instructions. Notably, upon the administration of antagomiR-21-5p, we observed an immediate and transient lethargic response in mice, lasting for approximately 10 minutes, although they subsequently recovered.

Glucose and insulin tolerance tests

The glucose tolerance test (GTT) was conducted following an overnight fasting period in male mice. Blood glucose levels were measured at 15, 30, 60, 90, and 180 minutes after intraperitoneal administration of 2 g/L glucose using a glucometer (ACCU CHEK Aviva III; Roche Diabetes Care). For the insulin tolerance test (ITT), mice were fasted for 4 hours. Subsequently, they received an intraperitoneal injection of 0.75 international units (IUs) of insulin (Lilly). Blood glucose levels were measured at 15, 30, 60, 90, and 180 minutes to evaluate glucose clearance in the blood.

Bone turnover markers

Following blood collection via heart puncture in our mouse model, the serum samples were collected in a 1.5 mL tube, clotted at room temperature for approximately 30 minutes, and centrifuged at 400 *g* for 10 minutes. All blood drawing were performed in the morning following at least 8 h of fasting. Serological analysis of bone turnover markers, specifically procollagen type 1 amino-terminal propeptide (P1NP) and tartrate-resistant acid phosphatase form 5b (TRAcP 5b). Within our human cohort, serum was obtained through peripheral blood collection. After a 30-minute clotting period at room temperature, the blood underwent centrifugation at 1200 *g* for 10 minutes. In the human T1DM case control study, all baseline blood samples were collected between 8 and 10 AM after an overnight fast. Clinical and laboratory parameter were measured as descried previously.[40,41] The resulting supernatant was then collected to assess osteocalcin (OCN) and C-terminal telopeptide (CTX) bone turnover markers. All bone turnover markers were conducted using commercially available ELISA kits obtained from IDS (Frankfurt/Main, Germany).

Bone microarchitecture analysis

The bone mass and microarchitecture of the distal femur and fourth lumbar vertebra (L4) were assessed using micro-computed tomography (microCT) with a vivaCT 40 scanner (Scanco Medical). Ex vivo scans of the bones were performed at an energy of 70 kVp and a resolution of 10.5 μm isotropic voxel size (114 mA, integration time 200 ms). One hundred slices from the distal femur and the mid-vertebra were analyzed using Scanco Medical standard protocols to evaluate trabecular bone parameters, including bone volume/-total volume (BV/TV), trabecular number (Tb.N), trabecular separation (Tb.Sp), trabecular thickness (Tb.Th), and trabecular bone mineral density (Tb. BMD). Additionally, cortical bone parameters, such as cortical thickness (Ct.Th) and cortical bone mineral density (Ct.BMD), were determined at the femoral midshaft. The femoral midshaft analysis also involved the analysis of 100 slices.

Bone immunohistochemistry

The L4 vertebrae and femoral bones were fixed in 4% PBS-buffered paraformaldehyde for 48 hours and subsequently decalcified using Osteosoft (Merck, Germany) for a period of 7 d. To prepare the samples for analysis, the bones underwent dehydration through a series of increasing ethanol concentrations before being embedded in paraffin. Thin sections measuring 2 μm were then obtained from the decalcified bones. Nrf2 immunohistochemistry was performed using an anti-Nrf2 antibody (#ab62352; Abcam) according to the manufacturer's instructions. The procedure involved applying a primary Nrf2 antibody (diluted 1:250) and subsequently treating it with a secondary antibody using the VECTASTAIN Elite ABC system (PK-6101; Vector laboratories) to enhance Nrf2 visualization. Quantification of the aforementioned parameter was carried out using the Microscope Axio Imager

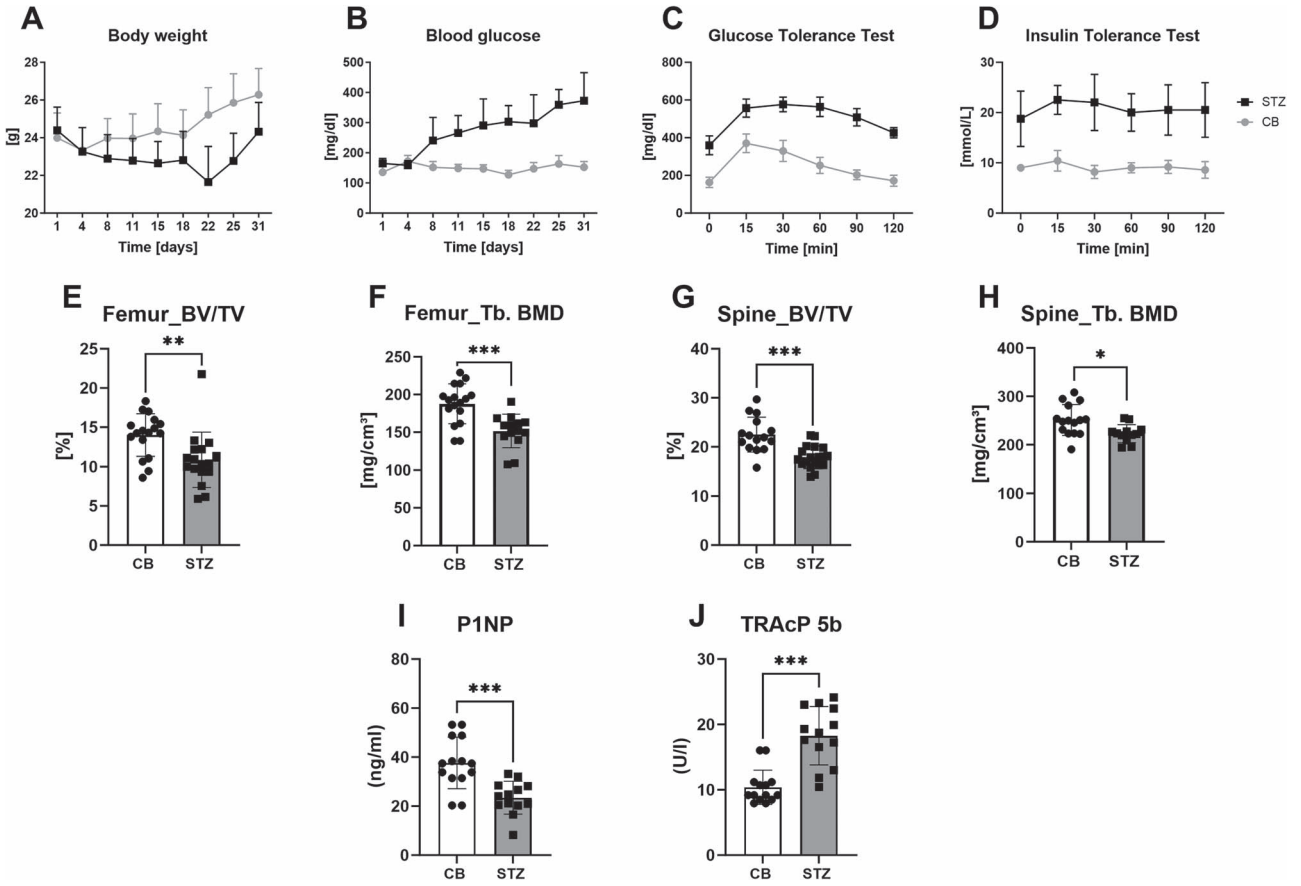

Figure 1. Decreased bone mass and formation in STZ-induced T1D mouse model. Body weight and blood glucose level were monitored from the beginning of the experiment until the end at 14 wk of age. Bone analysis and serum marker measurements in 14-wk-old male STZ-induced T1D (STZ) and their control littermates (CB). (A and B) Body weight and blood glucose level measurements. (C) A GTT and (D) ITT from 14-wk-old T1D (STZ) vs non-diabetic (CB) male mice was carried out. BV/TV and Tb.BMD were assessed using microCT for (E and F) femur and (G and H) and the fourth vertebral body. (I) Serum levels of the bone formation marker, P1NP, and (J) the bone resorption marker, TRAcP 5b were measured using ELISA. Data are presented as mean ± SD. Statistical analysis was performed using Student's *t*-test, and significance levels are denoted in the graphs as $^{*}P < .05$, $^{**}P < .01$, $^{***}P < .001$. $n = 13$ to 17 per group.

M1 (Carl Zeiss Jena) in conjunction with Osteomeasure software (OsteoMetrics). Nrf2-positive cells were quantified in the central region of bone tissue slices, covering a total area of 0.72 and 0.48 mm^2 for vertebrae and femoral bones, respectively. The quantification process adhered to the guidelines set forth by the Nomenclature Committee of the ASBMR.[42]

miRNA measurements in mouse samples

Total RNA was extracted from various tissues including bone, bone marrow, liver, pancreas, and tibia muscle using TRIzol reagent (Invitrogen) following the manufacturer's instructions. The RNA samples were then quantified using a Nanodrop ND-1000 spectrophotometer (Thermo Scientific/PEQLAB). Post-mortem, the femora and tibiae were collected without the ends of the bones and flushed with PBS prior to RNA extraction to exclude the bone marrow from further analysis. For miRNA reverse transcription, 5 nanograms of total RNA were used and reverse-transcribed using the miRCURY LNA RT Kit (#339340; Qiagen). Subsequently, the cDNA samples were diluted at a ratio of 1:40. Quantitative real-time PCR using miRCURY LNA SYBR Green (#339345; Qiagen) was conducted. The PCR conditions were as follow: 95°C for 2 minutes, followed by 95°C for 10 seconds and 56°C for 60 seconds, repeated 40 times. To normalize the data, the expression levels of miRNA were compared to the expression of the 5S housekeeping gene, observed to be the most suitable housekeeping gene for our samples, using the ΔΔCT method and are expressed as fold change (x-fold). All procedures were following the manufacturer's instructions.

mRNA–cDNA synthesis and quantitative real-time polymerase chain reaction (RT-PCR) for mouse samples

For mRNA reverse transcription, 500 nanograms of RNA were used, and the Superscript kit (Invitrogen) was employed. Subsequently, SYBR Green-based quantitative real-time PCR was performed. The primer sequences used for amplification are reported in Supplementary Table 1. The PCR cycling conditions consisted of an initial step at 50°C for 5 minutes, followed by 10 minutes at 95°C. This was followed by 40 cycles of 95°C for 15 seconds and 60°C for 1 minute. Melting curves were evaluated by using the following scheme: 95°C for 15 seconds, 60°C for 1 minute, and 95°C for 30 seconds. The results were calculated using the ΔΔCT method and are presented as a fold change normalized to the β-actin level.

Study population of T1DM

A cohort of adults with T1DM was recruited at the Department of Medicine and Clinic of Endocrinology and Nephrology at the University hospital of Leipzig, Germany in

the context of the Leipzig Obesity BioBank. T1DM patients and non-diabetic volunteers were matched based on age, sex, and body mass index (BMI). For this study, we enrolled 30 T1DM patients (15 women and 15 men) and 28 control individuals (15 women and 13 men), in the age group between 42 and 60 yr with a BMI range from 27.8 to 51.1 kg/m^2, indicative of an overweight/obesity cohort.

Patients diagnosed with T1DM displayed HbA1c levels between 6.0% and 7.2 %. All individuals in the control group fulfilled the following inclusion criteria: (1) fasting plasma glucose (FPG) <7.0 mmol/L; (2) HbA1c <6.0%; and (3) stable weight, defined as the absence of fluctuations of >2% of body weight for ≥3 mo before blood testing. In addition, the following exclusion criteria have been defined and applied to all study population: (1) medical and family history of T1DM or T2DM; (2) medical history of hypertension or systolic blood pressure >140 mmHg and diastolic blood pressure >85 mmHg; (3) any acute or chronic inflammatory disease, as determined by a leucocyte count >8000 Gpt/L, C-reactive protein >5.0 mg/dL, or clinical signs of infection; (4) clinical evidence of either cardiovascular or peripheral artery disease; (5) any type of malignant disease; (6) thyroid dysfunction; (7) Cushing's disease or hypercortisolism; (8) alcohol or drug abuse; (9) pregnancy.

Biological parameters including age and BMI, from both groups have been documented in Table 1. Blood samples taken after a minimum of 8 h of fasting were either analyzed immediately or centrifuged within 30 min and stored at −80°C within 2 h. The measured characteristics included BMI, HbA1c, FPG levels, OCN, CTX, and 25OHD concentrations. Additionally, serum samples were assessed for the detection of miR-144-5p and miR-21-5p. Ethical approval (Leipzig University approval no: 159-12-21052012) was secured for this study cohort adhering to the principles of the Helsinki Declaration. All participants gave written informed consent before taking part in the study.

miRNA measurements in human samples

Total RNA was extracted from human serum using the miRNeasy Mini Kit (Qiagen) following the manufacturer's protocol. For each sample, precisely 200 μL serum were mixed with 1000 μL Qiazol and 1 μL of a mix of 3 synthetic spike-in controls including UniSp4 (miRCURY spike-in kit, Qiagen, Cat No. 339390) by vortexing. Following 10-min incubation at room temperature, 200 μL chloroform were added to the lysates followed by centrifugation at 12 000 *g* for 15 minutes at 4°C. Precisely, 650 μL of the upper aqueous phase were transferred to a miRNeasy mini column where RNA was precipitated with 750 μL ethanol followed by automated washing with RPE and RWT buffer in a QiaCube liquid handling robot. Finally, total RNA was eluted in 30 μL nuclease-free water and stored at −80°C.

For cDNA synthesis, miRCURY LNA RT kit (Qiagen, Cat No. 339340) was used. RT reaction included 4 μl total RNA in a 10 μl volume. To monitor RT efficiency and presence of impurities with inhibitory activity, a synthetic RNA spike-in (cel-miR-39-3p) was added to the RT reaction. qPCR was performed in a Roche LC96I instrument (Roche). PCR conditions were: 42°C for 60 minutes, denaturation at 95°C for 5 minutes, and storage at 4°C. RT-PCR used miRCURY SYBR Green qPCR kit (Qiagen, Cat No. 339347) and miRCURY LNA miRNA PCR Assay products (Qiagen, Cat No. 339306).

Table 1. Characteristic of the study population.

	Both genders		**Women**		**Men**	
	Control (*n* = 27-30)	**T1D (*n* = 26-30)**	**Control (*n* = 14-15)**	**T1D (*n* = 12-15)**	**Control (*n* = 12-13)**	**T1D (*n* = 14)**
Biometric parameters						
Age (yr)	53.5 (42.0–59.5)	48.0 (42.0–60.0)	52.5 (38.0–58.3)	47.5 (36.7–48.7)	55.5 (52.3–62.3)	58.0 (41.0–61.8)
Body mass index (kg/m^2)	36.6 ± (27.8–43.8)	**41.3 ± (36.6–51.1)***	36.2 ± (28.7–44.6)	42.3 ± (36.8–50.6)	37.1 ± (26.7–45.5)	41.1 ± (36.0–51.5)
Serum parameters						
HbA1c (%)	5.50 ± (5.30–5.70)	7.00 ± (6.40–7.40)	5.40 ± (5.40–5.50)	7.20 ± (7.20–7.20)	5.50 ± (5.40–5.60)	6.70 ± (6.70–6.80)
Fasting plasma glucose (mmol/L)	5.30 ± (4.90–5.70)	**6.70 (5.80–7.50)*****	5.50 ± (4.90–5.80)	**6.70 (5.60–7.40)*****	5.20 ± (4.80–5.30)	**7.00 ± (5.80–7.70)*****
OCN (ng/mL)	11.8 ± (7.80–16.2)	**6.90 (3.70–12.5)****	10.5 ± (7.80–15.8)	**4.90 ± (3.30–10.7)***	12.3 ± (7.60–16.1)	7.60 ± (4.50–13.5)
CTX-I (ng/mL)	0.30 ± (0.10–0.40)	0.20 ± (0.10–0.30)	0.30 ± (0.10–0.50)	**0.10 ± (0.10–0.20)****	0.20 ± (0.10–0.30)	0.20 ± (0.10–0.30)
25OHD (ng/mL)	16.4 ± (10.5–29.8)	20.8 ± (13.7–23.8)	15.9 ± (11.3–27.3)	21.9 ± (20.3–28.4)	14.9 ± (10.3–28.0)	16.5 ± (10.2–23.0)

Note: Mean ± SD. Data are presented as the median along with the interquartile range (first to third quartiles). Significant variations are indicated by an asterisk as $^*P < .05$, $^{**}P < .01$, $^{***}P < .001$. Bold lines indicate significant differences.

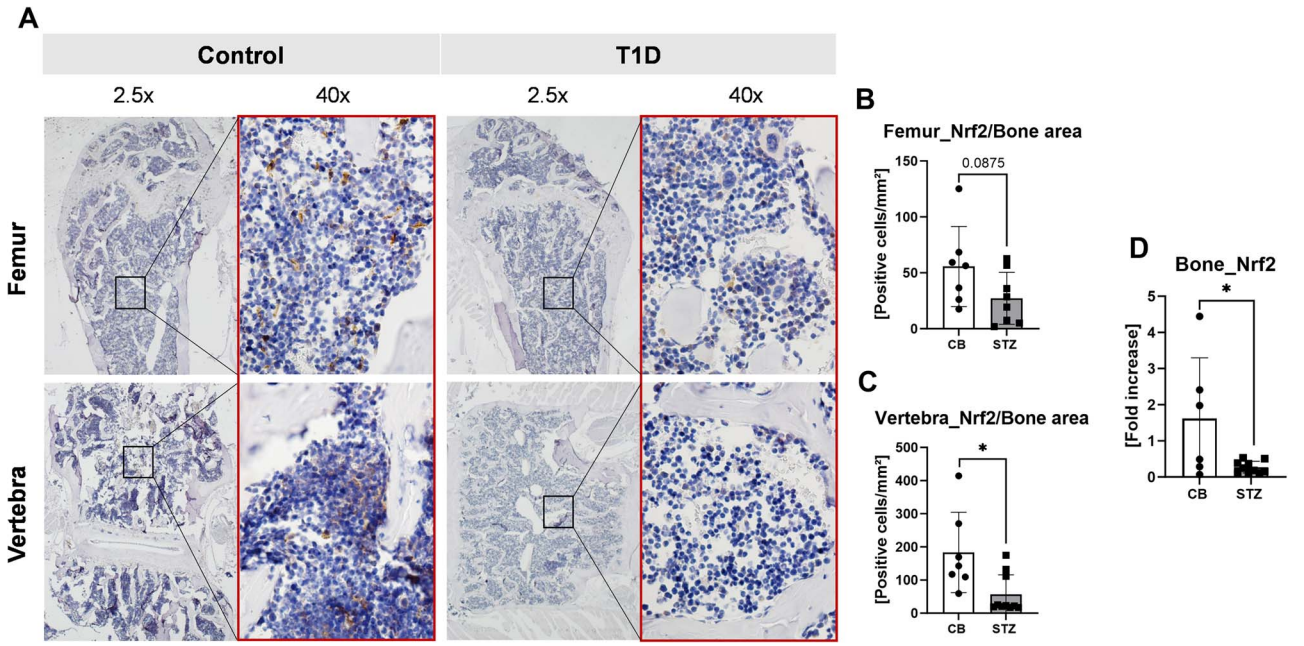

Figure 2. Downregulation of Nrf2 in STZ-induced T1D bone compared to control littermates. Femur and vertebra samples from 14-wk-old mice with STZ-induced T1D (STZ) and their control littermates (CB) were subjected to immunohistochemistry for quantifying Nrf2-positive stained cells in bone/bone marrow area (Nrf2/bone area). In (A), the upper line shows Nrf2 staining in the femur, while the second line shows Nrf2 staining in the vertebra bone. (B) Nrf2 quantification in the femur and (C) in the vertebra is shown by immunohistochemistry. (D) Nrf2 gene expression from bone was determined by qPCR. Data are presented as mean ± SD. Statistical analysis was performed using Student's *t*-test, and significance levels are denoted in the graphs as $^{*}P < .05$. $n = 6$ to 8 per group.

Results were analyzed using ΔΔCT method, expressed as fold change (x-fold), normalized to UniSp4 Spike-in.

Statistical analysis

The data are reported as mean SD. To compare 2 groups, a 2-sided, unpaired Student's *t*-test was conducted, while a one-way analysis of variance (ANOVA) using Tukey's multiple comparisons *post hoc* test was employed to evaluate the impact of antagomirs and T1DM interaction. All correlation analyses conducted on the human cohort were performed using Pearson correlation analysis. Outliers were identified using the Grubb's test. Graphs were generated using GraphPad Prism 9.0 software (GraphPad). Statistical significance was considered when the *P* value was less than .05.

Results

Decreased bone mass and bone formation in STZ-induced T1DM mouse model

We first examined the glucose and bone phenotype of our 14-wk-old mouse model with STZ-induced T1DM (STZ). Consistent with previous studies, we observed a decrease of the body weight and an increase of the blood glucose level in T1DM male mice compared to non-diabetic male mice, in a whole cohort of 14–17 per group (Figure 1A and B). Additionally, impairments in glucose tolerance and the ITT were observed in T1DM male mice compared to non-diabetic male mice during the evaluation (Figure 1C and D). Moreover, a reduction in bone volume and trabecular BMD in the distal femur of T1DM male mice (−23% and −19% respectively) was observed compared to their non-diabetic littermates (CB) (Figure 1E and F).[43] Moreover, a reduction was also detected in the fourth lumbar vertebrae (L4, −20% and −11%, respectively) (Figure 1G and H). Furthermore, we measured the serum levels of bone turnover markers in T1DM male mice and found a decrease in the bone formation marker P1NP (−38%), along with an increase in the bone resorption marker TRAcP 5b (+76%), compared to their non-diabetic littermates (Figure 1I and J). Thus, the STZ-induced mouse model of T1DM displayed the expected phenotype with femoral trabecular bone loss, reduced bone formation, and increased bone resorption.

Downregulation of Nrf2 in STZ-induced T1DM bone

As Nrf2 was recently reported to be downregulated in cardiac tissues from STZ-induced T1DM mice and in patients with T1DM,[44] we next examined Nrf2 protein expression in a subcohort of 6-8 per group, in bone of our T1DM male mice using immunohistochemistry. Using confocal microscopy, we observed a distinct disparity in Nrf2 staining in bone between non-diabetic and diabetic mice. We noticed a more prominent presence of Nrf2 (indicated by brown staining) in the femur and vertebral bones of non-diabetic male mice compared to T1DM male mice (Figure 2A). To substantiate this visual observation, we quantified the number of Nrf2-positive cells in both bone samples. The results showed a decreasing trend in Nrf2-positive cells in the femoral bone of T1DM male mice, with a reduction of 51% compared to the non-diabetic group (Figure 2B). Similarly, we observed a decrease in Nrf2-positive cells in the vertebra compartment of T1DM male mice, with a decrease of 69% (Figure 2C). To further investigate Nrf2 expression in the bone samples, we conducted qPCR analysis. Consistent with the immunohistochemistry findings, the qPCR data revealed an 83% decrease in Nrf2 expression in T1DM male mice compared to the non-diabetic group (Figure 2D).

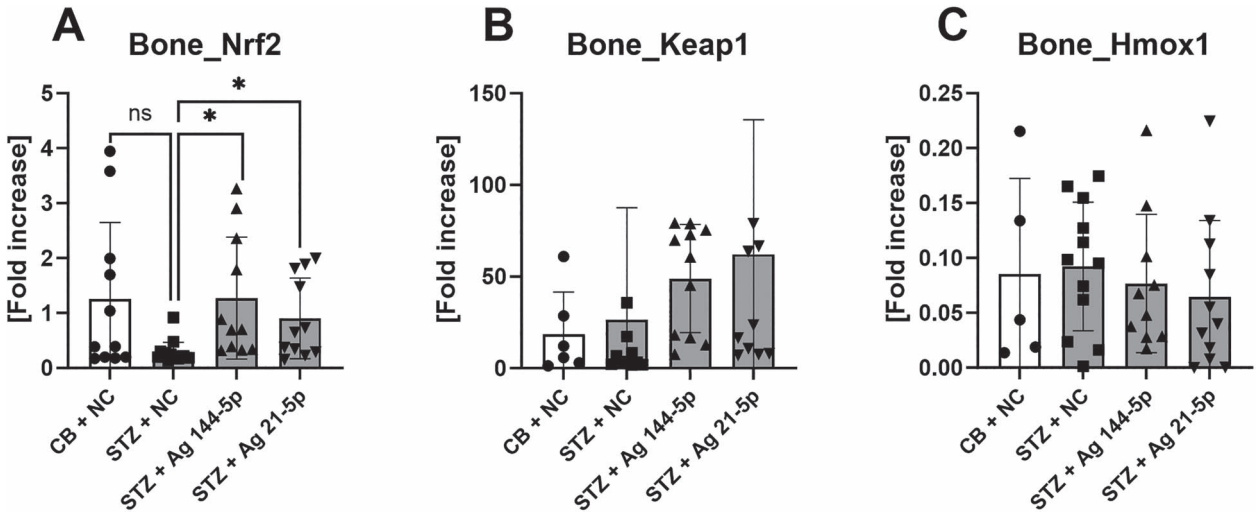

Figure 3. MiR-144-5p and miR-21-5p deletion improve Nrf2 expression in bone tissue. (A–C) Nrf2, Keap1, and Hmox1 associated to oxidative stress were measured by qPCR. Data are presented as mean ± SD. Statistical analysis was performed by one-way ANOVA using Tukey's multiple comparisons post hoc test. Statistical significance levels are denoted in the graphs as $^{*}P < .05$. $n = 5$ to 13 per group.

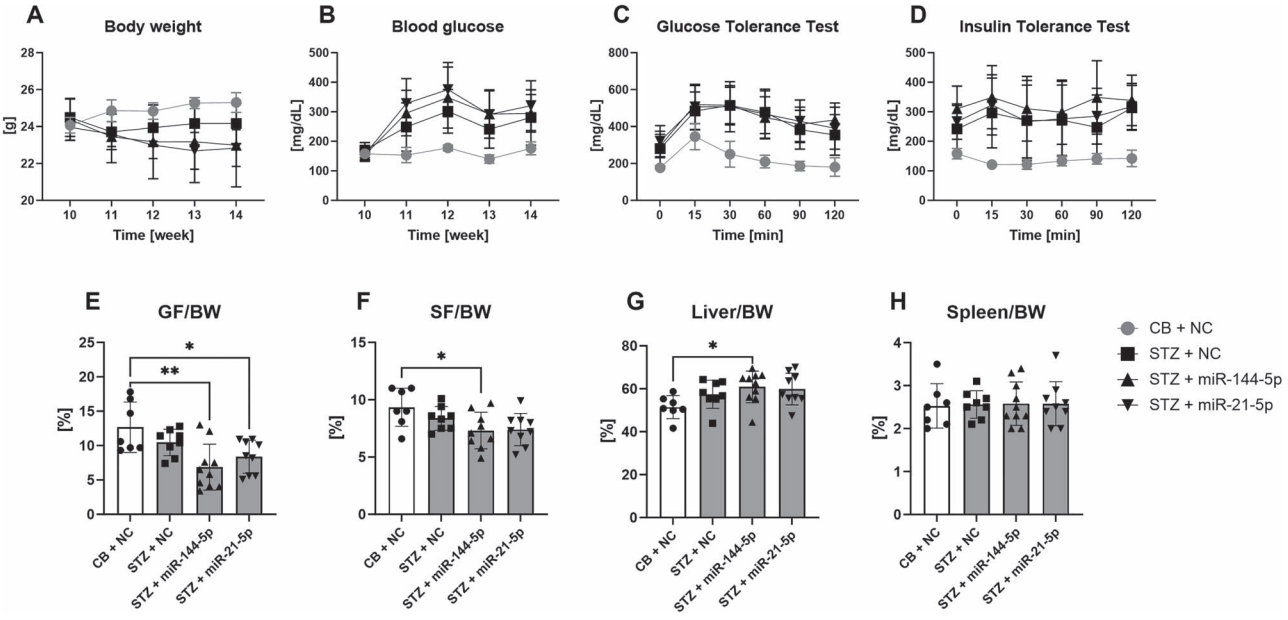

Figure 4. Decreased GF and SF in miR-144-5p knockdown, associated with increased liver weight in STZ-induced T1D male mice. All mice were fed a standard diet for 14 wk. (A) Body weight (BW) was measured, (B) a weekly blood glucose measurement from week 10 until the end of the experiment week 14, (C) a GTT and (D) ITT from 14-wk-old T1D (STZ + NC and STZ + miR-144-5p/miR-21-5p) vs non-diabetic (CB + NC) mice was carried out. Percentage of body (E) gonadal, (F) subcutaneous fat pads (GF, SF), and (G) liver and (H) spleen were quantified. Data are presented as mean ± SD. Statistical analysis was performed by one-way ANOVA using Tukey's multiple comparisons post hoc test. Statistical significance levels are denoted in the graphs as $^{*}P < .05$, $^{**}P < .01$. $n = 7$ to 10 per group.

Validation of miR-144-5p and miR-21-5p knockdown in T1DM male mice

As miR-144-5p and miR-21-5p target Nrf2 and have been reported to be increased in T1DM, we knocked down miR-144-5p and miR-21-5p down in STZ-induced T1DM male mice to investigate their role in diabetic bone disease. One week after reaching a diabetic status, T1DM received either antagomir-144-5p or antagomir-21-5p via intravenous injection. At 14-wk of age, we assessed the knockdown efficiency of each targeted miRNA in the bone, bone marrow, liver, and skeletal muscle. T1DM male mice receiving antagomirs showed a decreased level of miRNAs for the respective antagomirs given. T1DM male mice receiving antagomir-144-5p did not show an altered expression of miR-144-5p in bone tissue, but it was decreased in bone marrow, liver, and skeletal muscle compared to T1DM receiving scrambled antagomir treatment (NC, Supplementary Figure 1A–D). As for T1DM male mice receiving antagomir-21-5p, we observed a decreased level of miR-21-5p in bone, bone marrow, liver, and skeletal muscle compared to control T1DM mice (Supplementary Figure 1E–H). Additionally, we measured the level of miR-451a in bone, bone marrow, and liver to check for any off-target binding of the antagomirs. However, no off-target effects were observed (Supplementary Figure 1I–K).

In addition, we analysed Nrf2 expression in bone, as we hypothesized that knockdown of the 2 miRNAs would rescue Nrf2 levels in diabetic male mice. Indeed, although Nrf2 mRNA expression levels were markedly decreased in T1DM

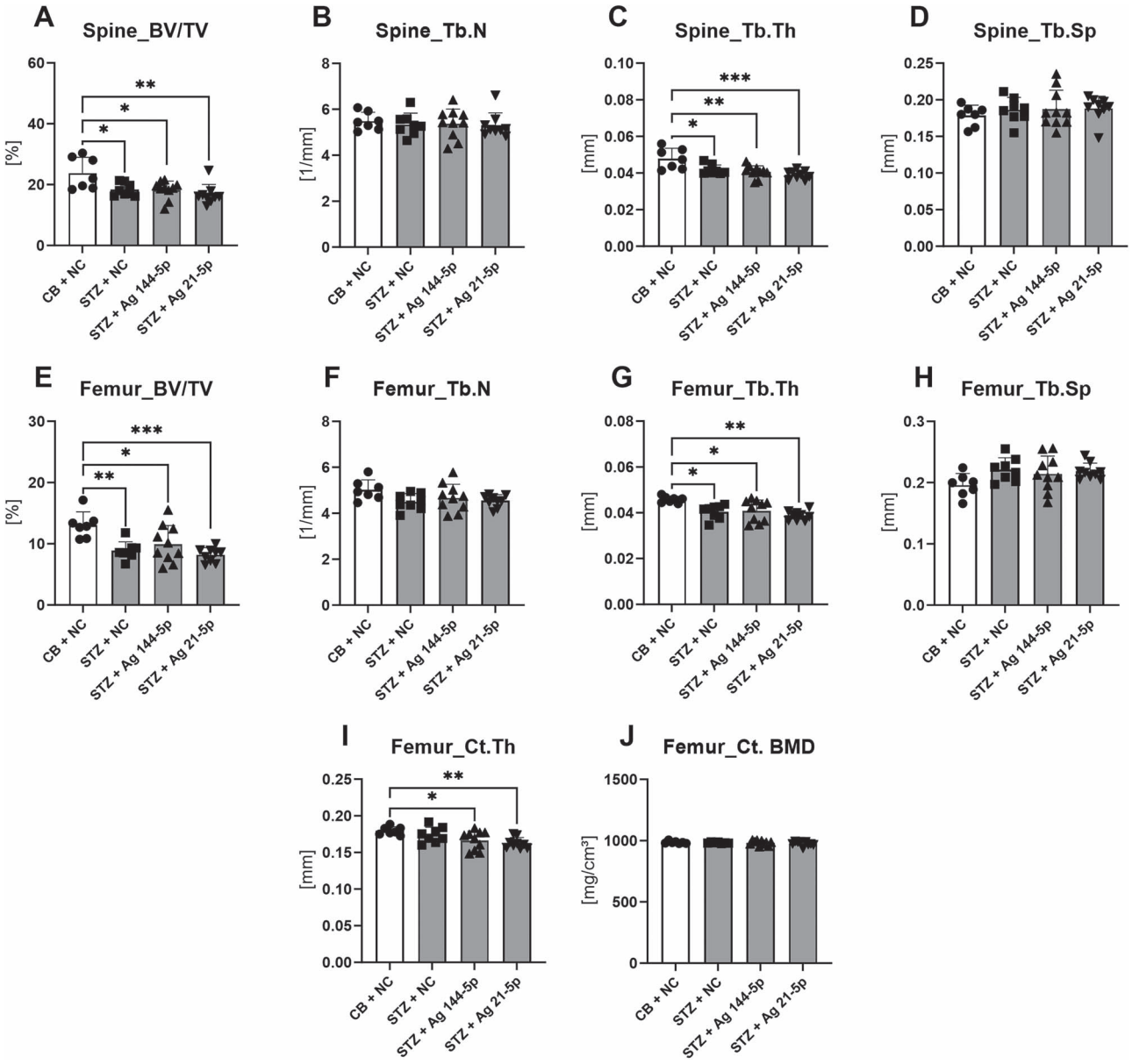

Figure 5. Inhibition of miR-144-5p and miR-21-5p does not protect against STZ-induced bone loss. Bones of 14-wk-old T1D (STZ + NC and STZ + miR-144-5p/miR-21-5p) and non-diabetic (CB + NC) were analyzed by microCT. (A) Bone volume per total volume (BV/TV), (B) trabecular number (Tb.N), (C) trabecular thickness (Tb.Th), and (D) trabecular seperation (Tb.Sp) of the fourth vertebral body. Additionally, (E) BV/TV, (F) Tb.N, (G) Tb.Th, (H) Tb.Sp at the distal femur, (I) cortical thickness (Ct.Th) of the femoral midshaft and (J) cortical bone mineral density (Ct.BMD) of the femoral midshaft. Data are presented as mean ± SD. Statistical analysis was performed by one-way ANOVA using Tukey's multiple comparisons post hoc test. Statistical significance levels are denoted in the graphs as $^{*}P < .05$, $^{**}P < .01$, $^{***}P < .001$. $n = 7$ to 10 per group.

male mice receiving the NC, treatment with both antagomirs normalized Nrf2 mRNA levels back to levels displayed by the non-diabetic male mice (Figure 3A). Keap1 and the Nrf2 target gene Hmox1 were, however, not altered by T1DM or the antagomir treatments (Figure 3B and C). Thus, these results confirm the successful knockdown of the miRNAs in the T1DM male mice and show that they can restore normal Nrf2 mRNA expression levels in diabetic bone.

Knockdown of miR-144-5p or miR-21-5p do not alter the development of T1DM

To evaluate the potential impact of miR-144-5p and miR-21-5p on the metabolic parameters of our T1DM mouse model, we closely monitored body weight and blood glucose levels throughout the experiment. Additionally, after culling, we measured the weights of the gonadal and subcutaneous fat pads, as well as the liver and spleen, relative to the total body weight. One week after the induction of T1DM using STZ, all T1DM male mice displayed a decrease in body weight (Figure 4A) and an increase in glucose levels (Figure 4B) compared to non-diabetic male mice. These effects persisted until the end of the experiment at 14 wk of age. At that time, T1DM treated with antagomirs even displayed a lower weight as compared to T1DM receiving the NC (Figure 1A). Finally, all T1DM displayed impaired glucose tolerance (Figure 4C) and insulin tolerance (Figure 4D), regardless of the antagomir treatment.

In line with the decreased body weight, T1DM male mice treated with antagomir-144-5p and -21-5p experienced a reduction in gonadal fat (−46% and −34% ,respectively)

when compared to non-diabetic male mice, but not compared to the T1D male mice with the NC antagomir (STZ + NC) (Figure 4E). Additionally, the subcutaneous fat of T1DM male mice treated with antagomir-144-5p exhibited a decrease compared to non-diabetic male mice (−22%), while the other diabetic groups did not show significant changes (Figure 4F). Interestingly, T1DM male mice treated with antagomir-144-5p displayed an increase in liver weight compared to non-diabetic male mice (+18%) (Figure 4G). We also assessed spleen weight but found no differences between the groups (Figure 4H). Taken together, the knockdown of miR-144-5p and miR-21-5p did not alter the course of T1DM development.

Inhibition of miR-144-5p and miR-21-5p does not protect against STZ-induced bone loss

We next examined the impact of antagomir-144-5p and -21-5p treatment on the bone characteristics of STZ-induced T1DM male mice using microCT analysis. In comparison to non-diabetic male mice, T1DM male mice in the control group (STZ + NC) and those treated with antagomir-144-5p and -21-5p exhibited lower bone volume in both L4 (−23%, −23%, −34%, respectively) and the distal femur (−32%, −24%, −37%, respectively) (Figure 5A and E). The reduction in vertebral and femoral bone volume was most pronounced in T1DM male mice treated with antagomir-21-5p. No significant alterations were observed in trabecular number (Figure 5B and F) or trabecular separation (Figure 5D and H) between the different groups in either the vertebrae or the femur. However, all T1DM male mice regardless of the antagomir treatment exhibited a lower trabecular thickness in the vertebrae (−13%, −15%, and −18%, respectively) and femur (−12%, −11%, and −15%, respectively) (Figure 5C and G). Furthermore, cortical thickness in the mid-shaft of the femur was lower in T1DM male mice treated with antagomir-144-5p and -21-5p compared to non-diabetic male mice (Supplementary Figure 2A). However, no changes were observed in cortical bone mineral density (Supplementary Figure 2B).

We next assessed whether the antagomir treatment had any effect on bone turnover. In terms of bone formation, both the T1DM NC group and the antagomir-treated male mice displayed a decrease in the serum levels of the bone formation marker P1NP (−46%, −52%, and −49%, respectively) compared to non-diabetic male mice (Figure 6A). In addition, the bone resorption marker TRAcP 5b was higher in T1DM male mice treated with antagomir-144-5p and -21-5p compared to the non-diabetic male controls (Figure 6B). Finally, we conducted gene expression analysis in bone tissue to evaluate the impact of antagomirs on osteogenic markers in male mice with T1DM. Rankl and Opg mRNA expression both tended to be increased in T1DM male mice, resulting in an unaltered Rankl/Opg ratio (Figure 7A–C). Moreover, as a characteristic feature of T1DM, Ocn levels were lower in T1DM male mice compared to non-diabetic male mice (Figure 7D). The antagomir treatment did not alter Ocn mRNA levels in T1DM male mice (Figure 7D). Additionally, alkaline phosphatase (Alpl) and type I collagen (Col1a1) expression were decreased in T1DM + NC male mice, but not in the T1DM male mice treated with miR-144-5p or miR-21-5p antagomirs (Figure 7E and F). Taken together, knockdown

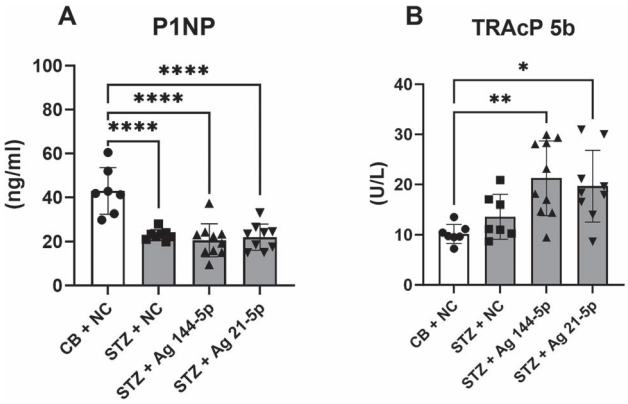

Figure 6. MiR-144-5p and miR-21-5p deletion does not improve bone formation nor reduced bone resorption in STZ-induced T1D male mice. Serum samples from 14-wk-old T1D (STZ + NC and STZ + miR-144-5p/miR-21-5p) and non-diabetic (CB + NC) mice were used for quantification of bone turnover markers. Serum level of (A) bone formation marker P1NP and (B) bone resorption marker, TRAcP 5b were measured using ELISA. Data are presented as mean ± SD. Statistical analysis was performed by one-way ANOVA using Tukey's multiple comparisons post hoc test. Statistical significance levels are denoted in the graphs as $^{*}P < .05$, $^{**}P < .01$, $^{****}P < .001$. $n = 7$ to 10 per group.

miR-144-5p or miR-21-5p does not improve diabetic bone disease in T1DM male mice.

miR-144-5p and miR-21-5p abundance is not altered in serum of patients with T1DM

As we could not confirm that knockdown of miR-144-5p or miR-21-5p altered the course of diabetes, we measured the abundance of the miRNAs in serum samples from patients with T1DM. In contrast to previous publications,[20-22] we could not find an increased expression of both miRNAs in patients with T1DM (Figure 8A and D). When separating the groups by sex, miR-144-5p levels were not different in women (Figure 8B), but tended to be increased in men with T1DM (Figure 8C). In contrast, miR-21-5p was downregulated in women with T1DM (Figure 8E), but was not altered in men with T1DM (Figure 8F). We next performed correlation analyses of the miRNAs with Hb1Ac and bone turnover markers. There was no correlation between miR-144-5p or miR-21-5p with HbA1c, OCN, or CTX (Figure 9A–F). Although miR-21-5p was downregulated exclusively in T1DM women, no significant correlations were observed with the HbA1c, OCN, and CTX markers (Supplementary Figure 3A). Similarly, T1DM men also displayed no correlations (Supplementary Figure 3B).

Discussion

In this study, we investigated the effects of miR-144-5p and miR-21-5p on bone loss in male mice with STZ-induced T1DM and evaluated their expression in serum from patients with T1DM. miR-144-5p and miR-21-5p are both known to target Nrf2 expression, a critical factor in the response to oxidative stress.[23-28] As Nrf2 has been found to be decreased in mouse models of T1DM, and both, miR-144-5p and miR-21-5p are reported to be upregulated in T1DM, we hypothesized that knocking down these miRNAs might protect from type 1 diabetic bone disease by enhancing Nrf2 expression.

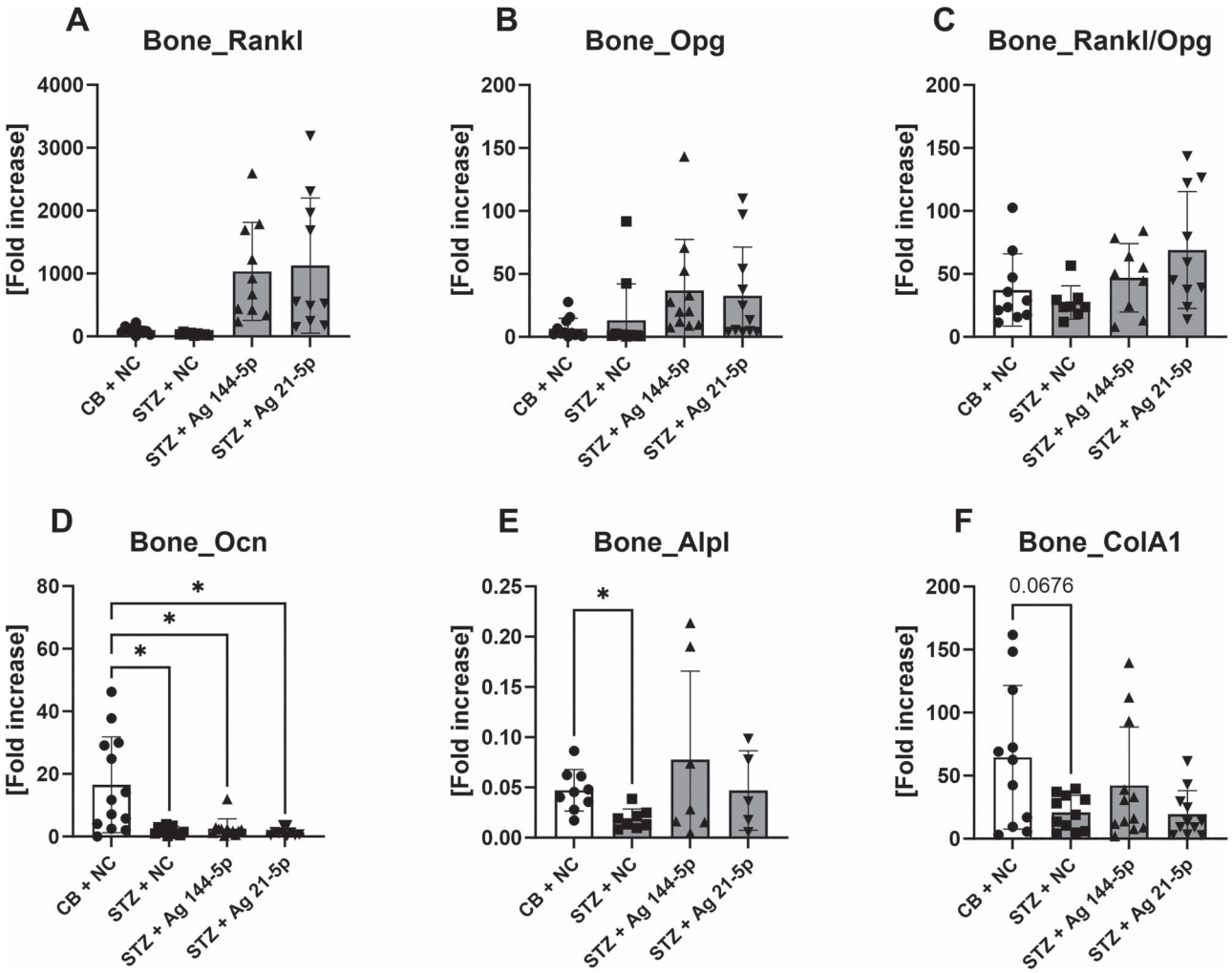

Figure 7. MiR-144-5p and miR-21-5p deletion does not improve osteogenic markers. Bones of all 14-wk-old mice were used for qPCR measurements. In the upper line (A–C), osteogenic markers were assessed for Rankl, Opg, and Rankl/Opg ratio, while in the second line (D–F), Ocn, Alpl, and Col1a1 associated to bone formation were assessed. Data are presented as mean ± SD. Statistical analysis was performed by one-way ANOVA using Tukey's multiple comparisons post hoc test. Statistical significance levels are denoted in the graphs as $*P < .05$. $n = 5$ to 13 per group. Abbreviation: Alpl , alkaline phosphatase; Col1a1, collagen, type I, alpha 1; Ocn, osteocalcin; Opg, osteoprotegerin.

Nrf2 is a well-known transcription factor involved in cellular responses and acts as a protector against oxidative stress.[45] Our findings indicate a reduction in Nrf2 expression in the bones of mice with T1DM, suggesting a potential link between T1DM-induced bone loss and diminished Nrf2 activity. These findings align with previous studies that highlight the protective effects of Nrf2 in STZ-induced T1DM mouse models.[46-48] Indeed, following therapeutic interventions aimed at activating or enhancing Nrf2 expression in the STZ-induced T1DM mouse model, the associated secondary complications of T1DM such as beta cell damage[46] and nephropathy[47,48] were attenuated through a reduction in oxidative stress, inflammation, and the release of cytokines. Despite the normalization of bone Nrf2 expression, knockdown of miR-144-5p and miR-21-5p did not rescue T1DM-induced bone loss. Treatment with antagomir-21-5p even appeared to exacerbate the reduction in bone volume, particularly in the vertebral trabecular and femoral cortical region. This was in line with persistently low levels of the bone formation marker P1NP in the serum and low expression of osteoblastic markers in bone, paired with an accentuated increase in the bone resorption marker TRAcP 5b in T1DM. These data led us to 3 hypotheses, potentially explaining why knockdown of these miRNAs did not ameliorate diabetic bone loss despite the rescue of Nrf2 expression: first, it could be that other targets of miR-144-5p and -21-5p might interfere with the protective effects of Nrf2 in diabetic bone disease. In fact, miR-21-5p has been shown to be a positive regulator of osteoblast differentiation and function, suggesting that its knockdown might impair osteoblast function.[49,50] Second, even though the mRNA expression of Nrf2 was restored in diabetic bone after antagomir treatment, Keap 1 expression, the negative regulator of Nrf2, tended to be increased suggesting an incomplete activation of Nrf2 in response to the antagomir treatment. This may go in line with the unchanged levels of Hmox1, one of the main targeted genes of Nrf2 with antioxidant and cytoprotective effects.[51] As we did not evaluate protein levels of this pathway, we cannot rule out the possibility that, despite normalized Nrf2 expression, the pathway was not fully activated in diabetic bone after the antagomir treatment. Third, Nrf2 might be eliciting a compensatory mechanism to protect against oxidative stress-induced damage. Nrf2 has been demonstrated to undergo activation in response to oxidative stress, particularly during acute and

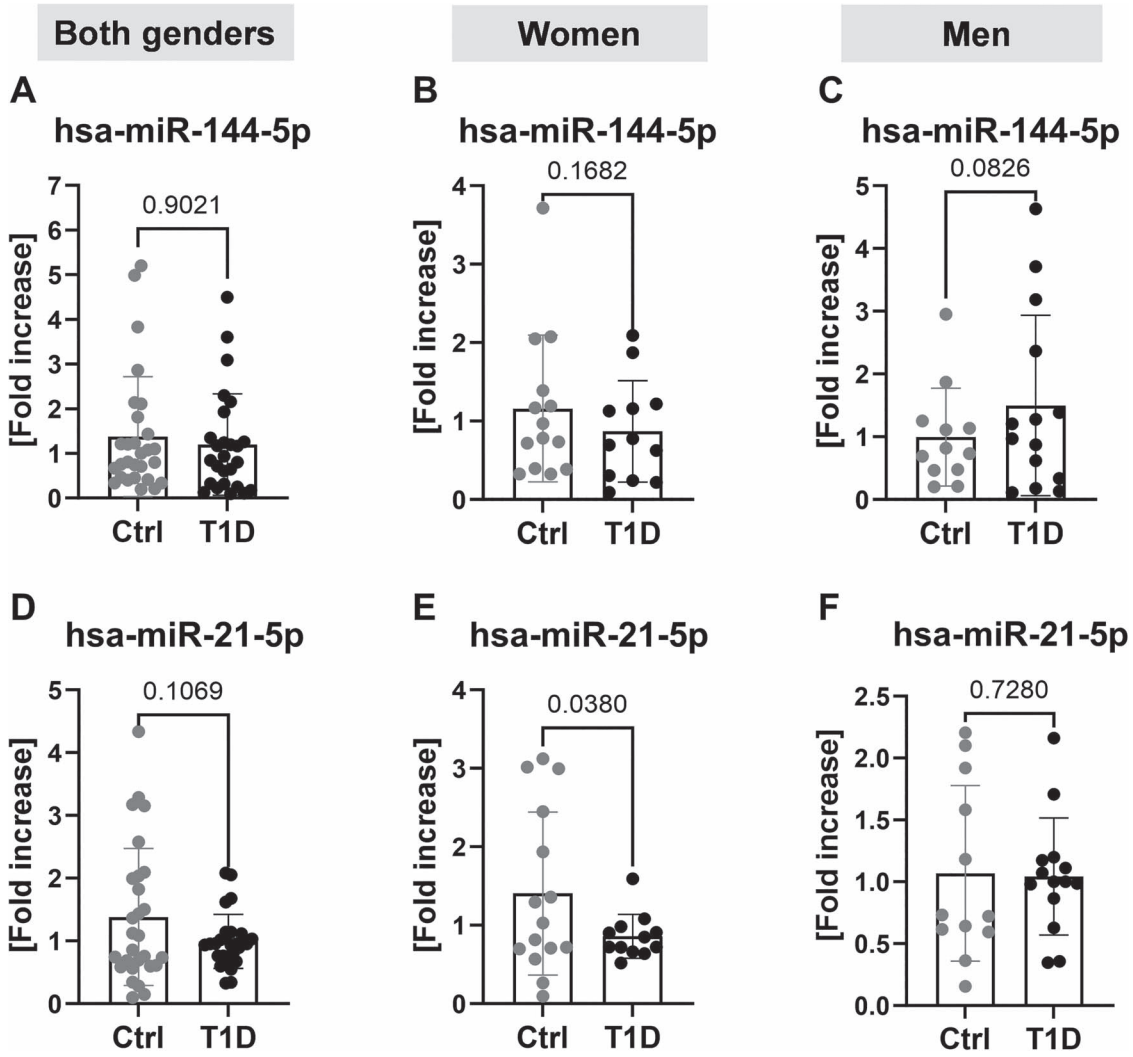

Figure 8. Comparative expression levels of miR-144-5p and miR-21-5p in T1D vs non-diabetic individuals. Serum samples from all participants were used for qPCR measurements. In the upper line (A–C), miR-144-5p was assessed in (A) both genders, (B) women, and (C) men, while in the subsequent row (D–F), miR-21-5p was evaluated in (D) both genders, (E) women, and (F) men. Ctrl (control group of non-diabetic individuals), T1D (type 1 diabetes subjects). Statistical analysis was performed using Student's *t*-test, and significance levels are denoted in the graphs as $P < .05$. $n = 12$ to 15 per group.

early stress phases. This phenomenon is well-documented in instances like cardiomyopathy in STZ-induced T1DM mice and T1DM-affected human cardiac tissues, where Nrf2 exhibited a noteworthy increase in activity within 2 mo of T1DM onset, followed by a subsequent decline after 5 mo.[44] In the context of T1DM, heightened Nrf2 expression within bone tissues of antagomirs treated T1DM mice may mirror a disruption in bone metabolism. Furthermore, despite remaining disparities surrounding the protective effects of Nrf2 on osteoblasts, evidence also indicates that activation of Nrf2 in primary osteoblasts[52,53] and MC3T3-E1 cells[54] is associated with a negative regulation of osteoblastogenesis. Taken together, these observations suggest that miR-144-5p and miR-21-5p do not play a crucial role in the development of diabetes or bone loss in T1DM mice, but also imply a complex interplay between our investigated miRNAs, oxidative stress, and bone in the context of T1DM.

Finally, we were unable to replicate the reported increase in miR-144-5p and miR-21-p expression in patients with T1DM. Possible differences in the study design and pre-analytics could have impacted the outcomes, such as the older age of our patients compared to other studies,[20-22] their quite obese status, and the disease stage. In particular, the disease status has been shown to be crucial when analyzing miRNAs. As such, miR-144-5p has been shown to be upregulated in children with T1DM at early disease stages, but not at later stages, and similarly, miR-144-5p was found to be upregulated in post-menopausal women with osteoporosis, but not with osteopenia.[20,55] Similar patterns were observed for miR-21 in plasma samples,[21] indicating potential disease-stage-related miRNA expressions. However, it should be noted that other studies also did not find an association of those miRNAs with parameters of diabetes control or bone turnover markers, suggesting only limited use of these miRNAs as biomarkers for diabetic bone disease.

Although this study provides significant insights, it has potential limitations. First, the study only included male mice, limiting the generalizability of the findings to both sexes. There are known sex-dependent differences due to sex hormones that may influence metabolic and bone outcomes.[56,57] Second, our study utilized a mouse model of T1DM induced by STZ, which offers valuable experimental advantages, but

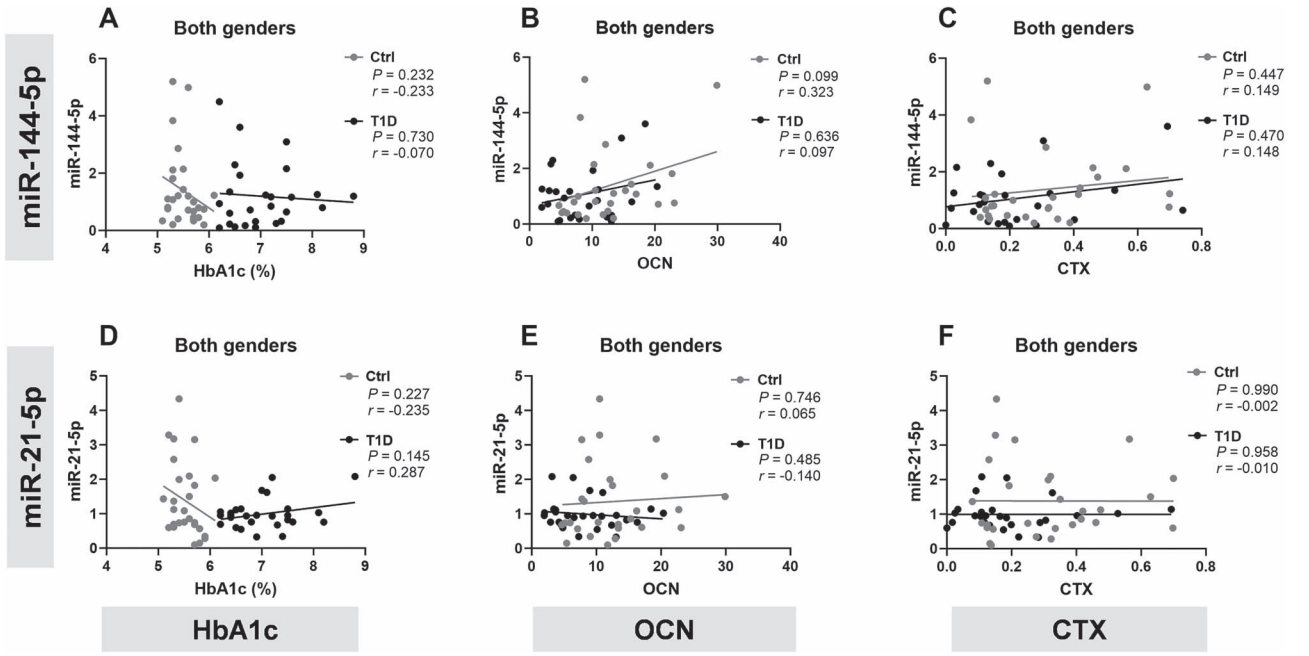

Figure 9. MiR-144-5p and miR-21-5p have no effect on HbA1c, nor on bone formation or bone resorption markers in T1D patients. Serum samples from all participants underwent HbA1c, OCN, and CTX measurements. Subsequent correlation analyses were conducted in T1D patients and control volunteers. In the upper panel (A–C), correlation analyses with miR-144-5p were performed with (A) HbA1c (%) level, (B) OCN, and (C) CTX markers. In the following row (D–F), identical analyses were performed for miR-21-5p. Here, no gender-based distinctions emerged, since no relevant variations were observed. The following annotations "*P*" indicates the *P*-value and "r" designates the Pearson correlation coefficient. Statistical analysis was performed using Pearson's correlation. $n = 28$ to 30 per group. HbA1c , hemoglobin A1c.

may not fully replicate all aspects of human T1DM or its treatment with insulin. The STZ-induced diabetic model is characterized by the development of insulitis, where the damage to β-cells is primarily attributed to the toxic effects of STZ rather than immune system dysregulation.[58] The frequency and dose of STZ administration could have influenced our outcomes. In our study, we deviated from the commonly employed one or 3-d STZ administration protocols used in previous studies prior to antagomir treatments[59,60] to achieve a complete penetrance of the phenotype. These deviations may have potentially exacerbated oxidative stress and altered the effects of antagomirs on the development of T1DM. Consequently, exploring alternative models would be beneficial to investigate the involvement of Nrf2 signaling specifically in autoimmune-based diabetes. Third, we were not able to collect data from the human cohort on diabetes duration or medication intake. Moreover, our cohort of patients with T1DM was rather old and obese, which makes the comparability to other studies usually performed in children and adolescents difficult. However, it also provides new insights into bone disease in obese patients with T1DM, which is a growing population.

Despite these limitations, our study has several strengths. We used a well-established mouse model of T1DM that provides a reliable platform for investigating the impact of Nrf2 and miRNA dysregulation on metabolic and bone parameters. Rigorous monitoring of key health parameters, including body weight and blood glucose levels ensured an accurate characterization. Furthermore, dose-finding experiments have been performed to identify the optimal dose of the antagomir for efficient miRNA knockdown. Also, the experiment was repeated in 2 independent cohorts with a substantial sample size, which strengthens the validity and reproducibility of the results. Most importantly, our study is the first to show the downregulation of Nrf2 in T1DM bone, representing a pioneering investigation into the miR-144-5p/Nrf2 and miR-21-5p/Nrf2 axis and bone loss in T1DM.

In conclusion, our study provides new insights into the impact of miR-144-5p and miR-21-5p on bone mass in STZ-induced T1DM mice. We show that silencing these miRNAs does not prevent bone loss in T1DM male mice or improve hyperglycemia. Further mechanistic studies focusing on the role of Nrf2 in T1DM-induced bone loss and strategies to enhance Nrf2 expression under diabetic conditions with more direct approaches might be useful to treat diabetic bone disease.

Acknowledgments

Thanks to H. Taipaleenmäki, LMU Munich, for her guidance regarding the use of antagomirs and M. Ledesma-Colunga, TU Dresden, for her for invaluable help in technical support with mice i.v. injections in this study.

Author contributions

Souad Daamouch (Conceptualization, Formal analysis, Investigation, Methodology, Project administration, Visualization, Writing – original draft, Writing – review & editing), Matthias Blüher (Resources), David Carro Vázquez (Methodology), Matthias Hackl (Resources, Software, Supervision, Writing – review & editing), Lorenz C. Hofbauer (Resources, Writing – review & editing), and Martina Rauner (Conceptualization, Investigation, Resources, Supervision, Writing – original draft, Writing – review & editing).

Supplementary material

Supplementary material is available at *JBMR Plus* online.

Funding

This study received financial support from the MARIE SKLODOWSKA-CURIE grant agreement no. 860898 ("FIDELIO"), which is part of the European Union's Horizon 2020 research and innovation program, and from the Elsbeth Bonhoff Stiftung.

Conflicts of interest

M.B. received honoraria as a consultant and speaker from Amgen, AstraZeneca, Bayer, Boehringer-Ingelheim, Lilly, Novo Nordisk, Novartis, and Sanofi. L.C.H. received honoraria as a consultant and speaker from Amgen, Novo Nordisk, and UCB and support for clinical trials from Ascendis. M.R. received honoraria as a speaker from UCB and Santhera. M.H. is CEO and cofounder of TAmiRNA GmbH. M.H. and D.C.V. are employees of TAmiRNA GmbH. S.D. has no conflict of interest.

Data availability

The data that support the findings of this study are available from the corresponding author upon reasonable request.

References

1. Powers AC. Type 1 diabetes mellitus: much progress, many opportunities. *J Clin Invest*. 2021;131(8):e142242. https://doi.org/10.1172/JCI142242
2. Maahs DM, West NA, Lawrence JM, Mayer-Davis EJ. Epidemiology of type 1 diabetes. *Endocrinol Metab Clin N Am*. 2010;39(3):481–497. https://doi.org/10.1016/j.ecl.2010.05.011
3. Zajec A, Trebušak Podkrajšek K, Tesovnik T, et al. Pathogenesis of type 1 diabetes: established facts and new insights. *Genes*. 2022;13(4):706. https://doi.org/10.3390/genes13040706
4. Primavera M, Giannini C, Chiarelli F. Prediction and prevention of type 1 diabetes. *Front Endocrinol*. 2020;11:248. https://doi.org/10.3389/fendo.2020.00248
5. Buzzetti R, Tuomi T, Mauricio D, et al. Management of latent autoimmune diabetes in adults: a consensus statement from an international expert panel. *Diabetes*. 2020;69(10):2037–2047. https://doi.org/10.2337/dbi20-0017
6. Hu J, Zhang R, Zou H, Xie L, Zhou Z, Xiao Y. Latent autoimmune diabetes in adults (LADA): from Immunopathogenesis to immunotherapy. *Front Endocrinol*. 2022;13:917169. https://doi.org/10.3389/fendo.2022.917169
7. Thomas NJ, Jones SE, Weedon MN, Shields BM, Oram RA, Hattersley AT. Frequency and phenotype of type 1 diabetes in the first six decades of life: a cross-sectional, genetically stratified survival analysis from UK Biobank. *Lancet Diabetes Endocrinol*. 2018;6(2):122–129. https://pubmed.ncbi.nlm.nih.gov/29199115/
8. Seyhan AA. microRNAs with different functions and roles in disease development and as potential biomarkers of diabetes: progress and challenges. *Mol Biosyst*. 2015;11(5):1217–1234. https://doi.org/10.1039/C5MB00064E
9. Hygum K, Starup-Linde J, Langdahl BL. Diabetes and bone. *Osteoporos Sarcopenia*. 2019;5(2):29–37. https://doi.org/10.1016/j.afos.2019.05.001
10. Sellmeyer DE, Civitelli R, Hofbauer LC, Khosla S, Lecka-Czernik B, Schwartz AV. Skeletal metabolism, fracture risk, and fracture outcomes in type 1 and type 2 diabetes. *Diabetes*. 2016;65(7):1757–1766. https://doi.org/10.2337/db16-0063
11. Vestergaard P. Discrepancies in bone mineral density and fracture risk in patients with type 1 and type 2 diabetes - a meta-analysis. *Osteoporos Int*. 2007;18(4):427–444. https://doi.org/10.1007/s00198-006-0253-4
12. Daamouch S, Emini L, Rauner M, Hofbauer LC. MicroRNA and diabetic bone disease. *Curr Osteoporos Rep*. 2022;20(3):194–201. https://doi.org/10.1007/s11914-022-00731-0
13. Ambros V. The functions of animal microRNAs. *Nature*. 2004;431(7006):350–355. https://doi.org/10.1038/nature02871
14. Zaidi SK, Young DW, Montecino M, et al. Bookmarking the genome: maintenance of epigenetic information. *J Biol Chem*. 2011;286(21):18355–18361. https://doi.org/10.1074/jbc.R110.197061
15. Kong Q, Guo X, Guo Z, Su T. Urinary exosome miR-424 and miR-218 as biomarkers for type 1 diabetes in children. *Clin Lab*. 2019;65(6). https://pubmed.ncbi.nlm.nih.gov/31232015/
16. Miao C, Chang J, Zhang G, Fang Y. MicroRNAs in type 1 diabetes: new research progress and potential directions. *Biochem Cell Biol*. 2018;96(5):498–506. https://pubmed.ncbi.nlm.nih.gov/29554441/
17. Satake E, Pezzolesi MG, Md Dom ZI, Smiles AM, Niewczas MA, Krolewski AS. Circulating miRNA profiles associated with Hyperglycemia in patients with type 1 diabetes. *Diabetes*. 2018;67(5):1013–1023. https://doi.org/10.2337/db17-1207
18. Lian JB, Stein GS, van Wijnen AJ, et al. MicroRNA control of bone formation and homeostasis. *Nat Rev Endocrinol*. 2012;8(4):212–227. https://doi.org/10.1038/nrendo.2011.234
19. Hackl M, Heilmeier U, Weilner S, Grillari J. Circulating microRNAs as novel biomarkers for bone diseases - complex signatures for multifactorial diseases? *Mol Cell Endocrinol*. 2016;432:83–95. https://doi.org/10.1016/j.mce.2015.10.015
20. Erener S, Marwaha A, Tan R, Panagiotopoulos C, Kieffer TJ. Profiling of circulating microRNAs in children with recent onset of type 1 diabetes. *JCI Insight*. 2017;2(4):e89656. https://doi.org/10.1172/jci.insight.89656
21. Seyhan AA, Nunez Lopez YO, Xie H, et al. Pancreas-enriched miRNAs are altered in the circulation of subjects with diabetes: a pilot cross-sectional study. *Sci Rep*. 2016;6(1):31479. https://doi.org/10.1038/srep31479
22. Grieco GE, Cataldo D, Ceccarelli E, et al. Serum levels of miR-148a and miR-21-5p are increased in type 1 diabetic patients and correlated with markers of bone strength and metabolism. *Noncoding RNA*. 2018;4(4):37. https://pubmed.ncbi.nlm.nih.gov/30486455/
23. La Sala L, Mrakic-Sposta S, Micheloni S, Prattichizzo F, Ceriello A. Glucose-sensing microRNA-21 disrupts ROS homeostasis and impairs antioxidant responses in cellular glucose variability. *Cardiovasc Diabetol*. 2018;17(1):105. https://doi.org/10.1186/s12933-018-0748-2
24. Jadeja RN, Jones MA, Abdelrahman AA, et al. Inhibiting microRNA-144 potentiates Nrf2-dependent antioxidant signaling in RPE and protects against oxidative stress-induced outer retinal degeneration. *Redox Biol*. 2020;28:101336. https://doi.org/10.1016/j.redox.2019.101336
25. Giacco F, Brownlee M. Oxidative stress and diabetic complications. *Circ Res*. 2010;107(9):1058–1070. https://doi.org/10.1161/CIRCRESAHA.110.223545
26. Narasimhan M, Patel D, Vedpathak D, Rathinam M, Henderson G, Mahimainathan L. Identification of novel microRNAs in post-transcriptional control of Nrf2 expression and redox homeostasis in neuronal, SH-SY5Y cells. *PLoS One*. 2012;7(12):e51111. https://doi.org/10.1371/journal.pone.0051111
27. Linna-Kuosmanen S, Tomas Bosch V, Moreau PR, et al. NRF2 is a key regulator of endothelial microRNA expression under proatherogenic stimuli. *Cardiovasc Res*. 2021;117(5):1339–1357. https://doi.org/10.1093/cvr/cvaa219
28. Sangokoya C, Telen MJ, Chi JT. microRNA miR-144 modulates oxidative stress tolerance and associates with anemia severity in sickle cell disease. *Blood*. 2010;116(20):4338–4348. https://doi.org/10.1182/blood-2009-04-214817
29. Baird L, Llères D, Swift S, Dinkova-Kostova AT. Regulatory flexibility in the Nrf2-mediated stress response is conferred by conformational cycling of the Keap1-Nrf2 protein complex. *Proc Natl Acad Sci U S A*. 2013;110(38):15259–15264. https://doi.org/10.1073/pnas.1305687110

30. McMahon M, Lamont DJ, Beattie KA, Hayes JD. Keap1 perceives stress via three sensors for the endogenous signaling molecules nitric oxide, zinc, and alkenals. *Proc Natl Acad Sci U S A*. 2010;107(44):18838–18843. https://doi.org/10.1073/pnas.1007387107
31. Yagishita Y, Uruno A, Chartoumpekis DV, Kensler TW, Yamamoto M. Nrf2 represses the onset of type 1 diabetes in non-obese diabetic mice. *J Endocrinol*. 2019;1:JOE-18-0355.R2.
32. Ding Q, Sun B, Wang M, et al. N-acetylcysteine alleviates oxidative stress and apoptosis and prevents skeletal muscle atrophy in type 1 diabetes mellitus through the NRF2/HO-1 pathway. *Life Sci*. 2023;329:121975. https://doi.org/10.1016/j.lfs.2023.121975
33. Han J, Yang K, An J, Jiang N, Fu S, Tang X. The role of NRF2 in bone metabolism - friend or foe? *Front Endocrinol*. 2022;13:813057. https://doi.org/10.3389/fendo.2022.813057
34. Zheng Y, Chen Z, She C, et al. Four-octyl itaconate activates Nrf2 cascade to protect osteoblasts from hydrogen peroxide-induced oxidative injury. *Cell Death Dis*. 2020;11(9):772. https://doi.org/10.1038/s41419-020-02987-9
35. Chen B, He Q, Yang J, et al. Metformin suppresses oxidative stress induced by high glucose via activation of the Nrf2/HO-1 Signaling pathway in type 2 diabetic osteoporosis. *Life Sci*. 2023;312:121092. https://doi.org/10.1016/j.lfs.2022.121092
36. Rai D, Tripathi AK, Sardar A, et al. A novel BMP2 secretagogue ameliorates glucocorticoid induced oxidative stress in osteoblasts by activating NRF2 dependent survival while promoting Wnt/β-catenin mediated osteogenesis. *Free Radic Biol Med*. 2022;190:124–147. https://doi.org/10.1016/j.freeradbiomed.2022.08.007
37. Zhao JW, Tang PJ, Zhou ZT, et al. Nrf2 signaling activation by a small molecule activator compound 16 inhibits hydrogen peroxide-induced oxidative injury and death in osteoblasts. *Cell Death Discov*. 2022;8(1):353. https://doi.org/10.1038/s41420-022-01146-7
38. Zhang D, Wu Y, Li Z, et al. MiR-144-5p, an exosomal miRNA from bone marrow-derived macrophage in type 2 diabetes, impairs bone fracture healing via targeting Smad1. *J Nanobiotechnology*. 2021;19(1):226. https://doi.org/10.1186/s12951-021-&break;00964-8
39. Furman BL. Streptozotocin-induced diabetic models in mice and rats. *Curr Protoc Pharmacol*. 2015;70:5.47.1–5.47.20. https://doi.org/10.1002/0471141755.ph0547s70
40. Milek M, Moulla Y, Kern M, et al. Adipsin serum concentrations and adipose tissue expression in people with obesity and type 2 diabetes. *Int J Mol Sci*. 2022;23(4):2222. https://doi.org/10.3390/ijms23042222
41. Klöting N, Fasshauer M, Dietrich A, et al. Insulin-sensitive obesity. *Am J Physiol Endocrinol Metab*. 2010;299(3):E506–E515. https://doi.org/10.1152/ajpendo.00586.2009
42. Dempster DW, Compston JE, Drezner MK, et al. Standardized nomenclature, symbols, and units for bone histomorphometry: a 2012 update of the report of the ASBMR Histomorphometry nomenclature committee. *J Bone Miner Res*. 2013;28(1):2–17. https://doi.org/10.1002/jbmr.1805
43. Hildebrandt N, Colditz J, Dutra C, et al. Role of osteogenic Dickkopf-1 in bone remodeling and bone healing in mice with type I diabetes mellitus. *Sci Rep*. 2021;11(1):1–10. https://doi.org/10.1038/s41598-021-81543-7
44. Tan Y, Ichikawa T, Li J, et al. Diabetic downregulation of Nrf2 activity via ERK contributes to oxidative stress-induced insulin resistance in cardiac cells in vitro and in vivo. *Diabetes*. 2011;60(2):625–633. https://doi.org/10.2337/db10-1164
45. Shaw P, Chattopadhyay A. Nrf2-ARE signaling in cellular protection: mechanism of action and the regulatory mechanisms. *J Cell Physiol*. 2020;235(4):3119–3130. https://doi.org/10.1002/jcp.29219
46. Song MY, Kim EK, Moon WS, et al. Sulforaphane protects against cytokine- and streptozotocin-induced beta-cell damage by suppressing the NF-kappaB pathway. *Toxicol Appl Pharmacol*. 2009;235(1):57–67. https://doi.org/10.1016/j.taap.2008.11.007
47. Cui W, Bai Y, Miao X, et al. Prevention of diabetic nephropathy by sulforaphane: possible role of Nrf2 upregulation and activation. *Oxidative Med Cell Longev*. 2012;2012:821936. https://doi.org/10.1155/2012/821936
48. Zheng H, Whitman SA, Wu W, et al. Therapeutic potential of Nrf2 activators in streptozotocin-induced diabetic nephropathy. *Diabetes*. 2011;60(11):3055–3066. https://doi.org/10.2337/db11-0807
49. Yang C, Liu X, Zhao K, et al. miRNA-21 promotes osteogenesis via the PTEN/PI3K/Akt/HIF-1α pathway and enhances bone regeneration in critical size defects. *Stem Cell Res Ther*. 2019;10(1):65. https://doi.org/10.1186/s13287-019-1168-2
50. Sikora M, Śmieszek A, Pielok A, Marycz K. MiR-21-5p regulates the dynamic of mitochondria network and rejuvenates the senile phenotype of bone marrow stromal cells (BMSCs) isolated from osteoporotic SAM/P6 mice. *Stem Cell Res Ther*. 2023;14(1):54. https://doi.org/10.1186/s13287-023-03271-1
51. Consoli V, Sorrenti V, Grosso S, Vanella L. Heme oxygenase-1 signaling and redox homeostasis in physiopathological conditions. *Biomol Ther*. 2021;11(4):589. https://doi.org/10.3390/biom11040589
52. Yoshida E, Suzuki T, Morita M, et al. Hyperactivation of Nrf2 leads to hypoplasia of bone in vivo. *Genes Cells*. 2018;23(5):386–392. https://doi.org/10.1111/gtc.12579
53. Sakai E, Morita M, Ohuchi M, et al. Effects of deficiency of Kelch-like ECH-associated protein 1 on skeletal organization: a mechanism for diminished nuclear factor of activated T cells cytoplasmic 1 during osteoclastogenesis. *FASEB J*. 2017;31(9):4011–4022. https://doi.org/10.1096/fj.201700177R
54. Hinoi E, Fujimori S, Wang L, Hojo H, Uno K, Yoneda Y. Nrf2 negatively regulates osteoblast differentiation via interfering with Runx2-dependent transcriptional activation. *J Biol Chem*. 2006;281(26):18015–18024. https://doi.org/10.1074/jbc.M600603200
55. Zhao SL, Wen ZX, Mo XY, et al. Bone-metabolism-related serum microRNAs to diagnose osteoporosis in middle-aged and elderly women. *Diagnostics*. 2022;12(11):2872. https://doi.org/10.3390/diagnostics12112872
56. Wenzel M, Pollow K. Reduction of androgens by (17-alpha-T)estradiol. *Hoppe Seylers Z Physiol Chem*. 1967;348:1667–1676. https://doi.org/10.1515/bchm2.1967.348.1.1667
57. Lorenzo J. Sexual dimorphism in osteoclasts. *Cells*. 2020;9(9):2086. https://doi.org/10.3390/cells9092086
58. Van Belle TL, Taylor P, von Herrath MG. Mouse models for type 1 diabetes. *Drug Discov Today Dis Models*. 2009;6(2):41–45. https://doi.org/10.1016/j.ddmod.2009.03.008
59. Wang Y, Yang LZ, Yang DG, et al. MiR-21 antagomir improves insulin resistance and lipid metabolism disorder in streptozotocin-induced type 2 diabetes mellitus rats. *Ann Palliat Med*. 2020;9(2):394–404. https://doi.org/10.21037/apm.2020.02.28
60. Li S, Chen X, Zhang H, et al. Differential expression of microRNAs in mouse liver under aberrant energy metabolic status. *J Lipid Res*. 2009;50(9):1756–1765. https://doi.org/10.1194/jlr.M800509-JLR200